Scale-Space Analysis of High-Speed Turbulent Flames

Aaron P. Jackson*, Alexei Y. Poludnenko, and Elaine S. Oran
Laboratories for Computational Physics and Fluid Dynamics
Naval Research Laboratory
Washington, DC, United States

1 Introduction

In this work, we analyze direct numerical simulations of three-dimensional (3D), freely propagating flames that are steadily driven by fast turbulence. Previous work has shown that these simulations belong to the thin reaction zone (TRZ) regime where the flamelet approximation is valid [1]. Our goal is to analyze the organization and evolution of the flame surface to identify patterns and features that may be used to construct subgrid-scale (SGS) models of turbulent premixed combustion. Namely, we wish to understand how flamelets are organized in the turbulent flame brush, whether a universal scaling law applies to the structure, over which scales the flame is folded, and whether the packing structure is stable.

Turbulent premixed combustion is a process that remains poorly understood, yet for most practical applications, we are forced to model this behavior. Previous studies of surfaces and mixing interfaces in turbulent flows suggest that the resulting structure is self-similar over a range of scales [2], which allow for its fractal description. Given the success experimental analyses have had identifying scaling relations of turbulent interfaces [3–5], SGS models for turbulent combustion have been constructed based on the assumption that the turbulent flame is self-similar on unresolved scales [6]. Nevertheless, this scaling behavior has not been demonstrated in the TRZ regime. In this regime, the smallest scale on which the flame is folded is limited by the laminar flame width rather than by the Gibson scale or Kolmogorov scale [7, 8].

2 Numerical Simulations

We have simulated turbulent premixed flames at two different turbulent intensities using the `Athena-RFX` code. The code solves the fully compressible, 3D reactive flow equations using a high-order fully conservative Godunov-type method based on the unsplit, corner-transport upwind algorithm. We use an ideal gas equation of state and model the chemical reaction rate of a H_2-air mixture using the single-step, first-order Arrhenius kinetics. The Lewis number is unity for both simulations. Simulations are conducted in a long channel with periodic boundary conditions orthogonal to the direction of flame propagation. Zero-gradient boundary conditions at either end of the domain prevent reflections and allow the flame

*National Research Council Research Associateship Program

to evolve freely. Turbulence is generated and sustained by injecting velocity perturbations at the largest scale of the flow to maintain a constant energy injection rate per unit volume. For a complete description of the method, see [1]. Tests have shown that 16 computational cells are required to resolve the laminar flame thermal width δ_L, where $\delta_L \equiv (T_b - T_u)/(\mathrm{d}T/\mathrm{d}x)_{\max}$ and T_b and T_u are the temperatures of the burned and unburned fuel, respectively.

The intensity of driven turbulence can be represented by the magnitude of the velocity fluctuations U_L at the scale of the domain L. Equivalently, one can distinguish different cases by using the turbulence velocity at the scale δ_L given by U_δ to compare to the laminar flame speed S_L. We consider two cases that highlight differences arising from the effect of the flame on turbulence: `Hv2` at $U_\delta = 2S_L$ and `Hv25` at $U_\delta = 25S_L$. The domain width is $L = 16\delta_L$. The flame is ignited at $t_0 = 0$ after two large-scale eddy turnover times (τ_{ed}), during which turbulence is allowed to equilibrate. We calculate time-averages between $t_1 = 2\tau_{\mathrm{ed}}$ and t_2 for the normalized quantities given in Table 1: the turbulent flame brush width, δ_T, normalized by L, the turbulent flame speed, S_T, normalized by S_L, the isosurface area, $A_{0.15}$, corresponding to the peak reaction rate $Y = 0.15$ normalized by L^2, the inverse flame surface density, $\Sigma_{0.15}^{-1}$, normalized by δ_L, and the inverse mean absolute value of curvature, $|\kappa_{0.15}|^{-1}$, normalized by δ_L. On average, the smallest scale on which the flame is wrinkled is of order $|\kappa_{0.15}|^{-1}$, while the average separation between flamelets within the flame brush is of order $\Sigma_{0.15}^{-1}$.

Table 1: Time-averaged properties of the turbulent flame brush.

	U_L	U_δ	t_2	$\overline{\delta_T/L}$	$\overline{S_T/S_L}$	$\overline{A_{0.15}}/L^2$	$\overline{\Sigma_{0.15}\delta_L}^{-1}$	$\overline{\lvert\kappa_{0.15}\rvert\,\delta_L}^{-1}$
`Hv2`	$5.04S_L$	$2S_L$	$10\tau_{\mathrm{ed}}$	2.0	4.8	4.7	7.0	2.86
`Hv25`	$63.0S_L$	$25S_L$	$6\tau_{\mathrm{ed}}$	2.54	8.9	6.9	8.4	1.09

In the higher-speed simulation `Hv25`, turbulence is faster than the flame on all scales, i.e. the Gibson scale is much smaller than δ_L. While the preheat zone is broadened, the reaction zone is not significantly affected by turbulence [1,9]. After $t = 6\tau_{\mathrm{ed}}$, the flame begins to transition to a detonation [10]; therefore, we are limited to only $4\tau_{\mathrm{ed}}$ to perform time averages. The average inverse curvature of the front is $\approx \delta_L$ signifying intense wrinkling. The lower-speed simulation `Hv2` shows the average inverse curvature to be $\sim 3\delta_L$. At scales close to δ_L, the flame speed is comparable to the turbulent fluctuations, and a more complex interplay between the flame and turbulence is observed. A cyclic pattern develops in the flame speed and flame surface area.

3 Methods

Straightforward methods to describe the scale-space flame surface structure, such as a Fourier decomposition, are not possible because the flame surface cannot be described as a simple height function. In the TRZ regime, the flame structure is complex with multiple surface-crossings in each direction. Two analysis methods were developed to study the time-dependent turbulent flame structure in scale space. Section 3.1 describes the direct sampling method that measures the average flame surface contained in a specific volume on different scales. Section 3.2 describes the diffusion method that smooths the flame surface on progressively larger scales. Both methods require a specific value of the fuel mass fraction Y to construct an isosurface for analysis. The isosurface corresponding to the peak reaction rate best describes the "flame surface."

3.1 Direct Sampling

In the case of direct sampling, we calculate the average surface area $\langle A_\lambda \rangle$ contained within a cubic volume of a given size λ. We find the surface area of an isosurface of Y using the "Marching Cubes" algorithm [11]. The scaling law, or fractal dimension D, can be estimated from a linear regression of $\log \langle A_\lambda \rangle$ as a function of $\log \lambda$. This scaling behavior describes how the surface area grows with length scale. A planar surface is described by $D = 2$, while $D = 3$ corresponds to a space-filling surface. The log-log derivative of $\langle A_\lambda \rangle$ with respect to λ provides a local fractal dimension $D = \partial \log \langle A_\lambda \rangle / \partial \log \lambda$. In this way, we can determine different scaling relations for different length scales, if they exist.

Our implementation of this sampling method is based on the "box-counting" algorithm. We construct a grid of cubes of arbitrary size λ, which may not divide evenly into the domain size. The simulations have periodic boundary conditions in the directions orthogonal to flame propagation, while the direction parallel is zero-gradient. In order to accurately measure $\langle A_\lambda \rangle$, we define two planes with normals parallel to the direction of propagation that constrain the analysis. These planes are chosen to encompass the volume in which $\xi <= Y <= 1 - \xi$, where $\xi = 10^{-6}$. Since for a given box size λ, the grid of boxes may not align with the constrained volume, a decision must be made of how to treat boxes that intersect the volume bounds. For the periodic boundaries, surface in the box is filled appropriately and counted normally; however, for the non-periodic boundaries, they are discarded.

We expect that $\langle A_\lambda \rangle$ should grow with λ as long as λ is smaller than the largest scale in the system, either L or δ_T; however, this method does not guarantee that $\langle A_\lambda \rangle$ is monotonic with λ. Non-monotonic behavior may be observed due to the statistical nature in which the averages are estimated; therefore, we use a large number of grid offsets to increase the number of boxes sampled to obtain a converged $\langle A_\lambda \rangle$. The total number of offsets is scaled with the box size, such that $N_{\text{offsets}} \approx 10\lambda^\beta$. We found $\beta = 1$ appropriate to adequately sample the surface. We compute $\langle A_\lambda \rangle$ by averaging all *surface-containing* boxes at scale λ across different grid offsets. Boxes that do not contain any surface area do not contribute to $\langle A_\lambda \rangle$.

3.2 Diffusion

We also analyze the scaling behavior of the flame surface with a completely different and complementary method that uses Gaussian convolution as a scale-dependent filter to smooth out small-scale features. The scaling behavior may be found by comparing the area of an isosurface smoothed on different scales. By differencing the area computed on two different smoothing scales, we determine how much surface area was contributed between those two smoothing length scales. Gaussian smoothing also guarantees that computed surface areas are monotonically decreasing with increasing λ. By smoothing the surface on progressively larger scales, the surface A_λ decreases with λ, a behavior different from the direct sampling method. For this method, we compute the scaling exponent $d = -\partial \log A_\lambda / \partial \log \lambda^2$, where d is theoretically related to the local fractal dimension by $d = (D - 2)/2$. This relation may not hold in practice due to the limited accuracy of the method or when the surface is not fractal.

Gaussian filtering can be recast as the solution of the diffusion equation. At each end of the flame brush along the direction of propagation, Y is well-defined as either 0 (products) or 1 (reactants). Directions perpendicular to the direction of propagation are periodic. We utilize Dirichlet boundary conditions to keep the fuel and ash states fixed at the boundaries of the domain and allow all isosurfaces to be reconstructed for any smoothing scale.

As with the direct sampling method, the analysis is limited to the volume in which $\xi <= Y <= 1 - \xi$, with $\xi = 10^{-6}$. Given an initial scalar field Y, a new scalar field smoothed on scale λ is computed using

discrete Fourier transforms with `FFTW 3.3`. An isosurface is constructed for a particular value of Y and its surface area is estimated using the "Marching Cubes" algorithm [11].

We have determined that this method is best suited for identifying local deviations in the scaling behavior of surfaces. In particular, this method identifies scale-space features that evolve dynamically in the system. Due to the underlying diffusion operation, however, the smoothing scale λ at which these features exist is different from the box size in the direct-sampling method.

4 Results

We analyze a large number of instantaneous snapshots of the scalar field. Several eddy turnover times are analyzed for each simulation with both the diffusion method and the direct sampling method. Figure 1 shows the results of applying the diffusion method, from which we can determine the evolution of localized structures in the flame brush. The color scale shows the log-log derivative d as a function of length scale and time in the top panel along with S_T and $A_{0.15}$ in the bottom panel. As turbulence distorts the flame, $\Sigma_{0.15}$ and $|\kappa_{0.15}|$ quickly saturate to a value typical for the turbulent intensity of the flow on a timescale much faster than τ_{ed}. As turbulence continues to distort the flame, the scale-space analysis indicates that wrinkling tends to be well-localized in scale space for simulation `Hv2`. On the other hand, simulation `Hv25` shows relatively uniform wrinkling in scale space. These observations are consistent with volume-rendered images of the flame brush. Simulation `Hv2` shows a flame whose width oscillates with the appearance and disappearance of large-scale structures that extend to a few times the domain width, while simulation `Hv25` shows a relatively steady flame width that is highly wrinkled on all scales.

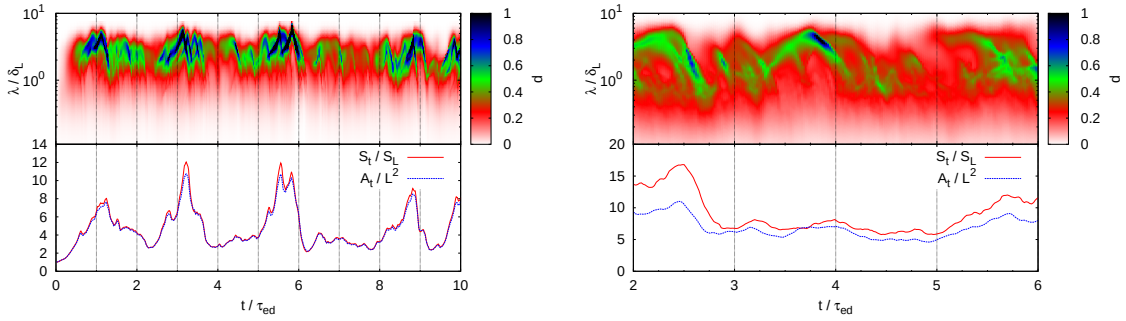

(a) Simulation `Hv2`. (b) Simulation `Hv25`.

Figure 1: The color scale shows d as a function of λ/δ_L and t/τ_{ed} in the top panel. The bottom panel shows S_T/S_L (solid red line) and $A_{0.15}/L^2$ (solid blue line) on the same time axis.

While the individual snapshots of the simulation demonstrate the evolution and dynamics of this system, we also wish to characterize the time-averaged scaling behavior of the flame surface. Figure 2 shows the time-averaged profiles of d and D for three different isosurface contours from the diffusion method and direct sampling method for each simulation. Time averages are performed over the same time interval as indicated in Table 1. By first comparing the diffusion method results between each simulation in Figures 2a and 2c, we qualitatively see that the higher-speed simulation `Hv25` populates a larger range of scales with wrinkles on average than the lower-speed simulation `Hv2`, which is consistent with the average separation between $|\kappa_{0.15}|^{-1}$ and $\Sigma_{0.15}^{-1}$. Burning has a stronger effect on the suppression of small-scale structures in the lower-speed simulation, which is consistent with previous studies [9]. Furthermore, burning in simulation `Hv2` appears to enhance larger-scale structures. The $Y = 0.9288$ isocontour from the higher-speed simulation is the only isosurface that shows evidence of self-similarity

over a significant range of scales. This isosurface corresponds to the preheat zone where we expect turbulence to dominate transport effects. Previous studies of turbulent interfaces have observed $D \approx 2.4$ [2], which is consistent with our results.

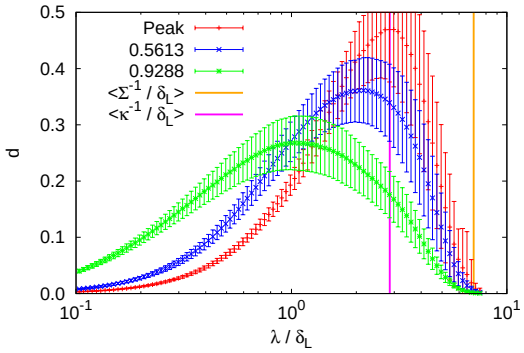

(a) Diffusion method results for Hv2.

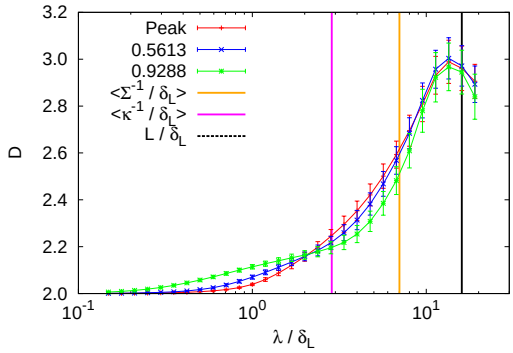

(b) Direct sampling method results for Hv2.

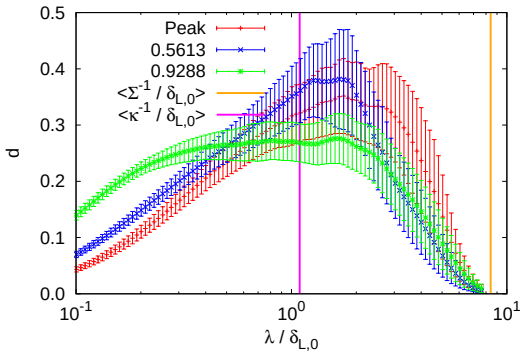

(c) Diffusion method results for Hv25.

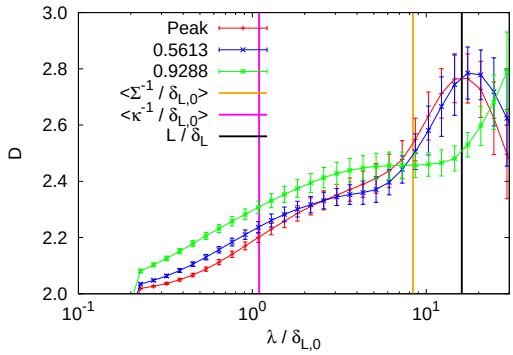

(d) Direct sampling method results for Hv25.

Figure 2: Time-averaged scale-space results from both methods for simulations Hv2 and Hv25. The left figures 2a and 2c show the time-averaged d from the diffusion method as a function of λ/δ_L for isosurface values of $Y = 0.1574$ (red), $Y = 0.5613$ (blue), and $Y = 0.9288$ (green). The upstream, fuel-side of the flame brush is represented by $Y = 1$, while the downstream, ash-side is $Y = 0$. The peak energy-generation rate occurs at $Y = 0.1574$, the isosurface of which most accurately represents the flame surface area. The right figures 2b and 2d show the time-averaged D from the direct sampling method as a function of λ/δ_L for the same values of Y. The error bars in all figures represent the standard error of the mean. For reference, $\overline{\Sigma_{0.15}^{-1}}/\delta_L$ (orange) shows the average separation between flamelets and $\overline{|\kappa_{0.15}|^{-1}}/\delta_L$ (magenta) shows the smallest average scale of wrinkling of the front.

The results from the direct sampling method in Figures 2b and 2d support similar conclusions: burning suppresses small-scale structures and the only isosurface that demonstrates self-similar behavior is $Y = 0.9288$ from simulation Hv25. Even though small-scale structures are suppressed, the higher-speed simulation still shows evidence of structure below δ_L, which is consistent with a broadened preheat zone. For $\lambda \gtrsim L$, the scaling behavior is not well-defined. The periodic boundary conditions impose some self-similarity for $\lambda \gtrsim L$, and δ_T oscillates around L. As λ grows above δ_T, $\langle A_\lambda \rangle$ will decline.

Some enhancement of large-scale structures is observed for the lower-speed simulation, but the measured effect on the scaling exponent is much smaller. In the higher-speed simulation, enhancement is only observed for $\lambda > \langle \Sigma_{0.15}^{-1} \rangle$, which is too close to L to attribute the enhancement to burning. The shape of the scaling exponent shifts systematically from a relatively flat profile in the preheat zone to a

monotonically increasing profile in the reaction zone.

5 Conclusions

We analyzed two different intensities of turbulent premixed combustion. In the high-speed case, we observed self-similar structures in the preheat zone, but none in the reaction zone. This shows that the reaction affects structures in scale space differently and breaks scale self-similarity. In the lower-speed case, the particular mechanism by which turbulence stretches the flame leads to cyclical behavior in the flame structure, that when time-averaged, does not constitute a self-similar structure.

Due to the limited range of scales that are accessible in simulations with modern computational resources, the extent of the influence of burning on large-scale structures is unclear. In order to test whether burning only affects a limited range of scales near δ_L or all scales through a backscatter process, we need to study a domain with L larger by an order of magnitude. Not only would such a study require significant computational resources, tests have shown that the likelihood of detonation increases with system size for fixed U_δ. Future studies aim to extend the present analysis to simulations larger domains while avoiding regimes that lead to deflagration-to-detonation transitions.

References

[1] A. Poludnenko and E. Oran, "The interaction of high-speed turbulence with flames: Global properties and internal flame structure," *Combust. Flame*, vol. 157, no. 5, pp. 995–1011, 2010.

[2] K. Sreenivasan, "Fractals and multifractals in fluid turbulence," *Annu. Rev. Fluid Mech.*, vol. 23, no. 1, pp. 539–604, 1991.

[3] K. Sreenivasan and C. Meneveau, "The fractal facets of turbulence," *J. Fluid Mech.*, vol. 173, no. 1, pp. 357–386, 1986.

[4] J. Mantzaras, P. Felton, and F. Bracco, "Fractals and turbulent premixed engine flames," *Combust. Flame*, vol. 77, no. 3, pp. 295–310, 1989.

[5] G. North and D. Santavicca, "The fractal nature of premixed turbulent flames," *Combust. Sci. Technol.*, vol. 72, no. 4-6, pp. 215–232, 1990.

[6] F. Gouldin, "An application of fractals to modeling premixed turbulent flames," *Combust. Flame*, vol. 68, no. 3, pp. 249 – 266, 1987.

[7] A. Kerstein, "Fractal dimension of turbulent premixed flames," *Combust. Sci. Technol.*, vol. 60, no. 4-6, pp. 441–445, 1988.

[8] Ö. Gülder and G. Smallwood, "Inner cutoff scale of flame surface wrinkling in turbulent premixed flames," *Combust. Flame*, vol. 103, no. 1, pp. 107–114, 1995.

[9] P. E. Hamlington, A. Y. Poludnenko, and E. S. Oran, "Interactions between turbulence and flames in premixed reacting flows," *Phys. Fluids*, vol. 23, no. 12, p. 125111, 2011.

[10] A. Poludnenko, T. Gardiner, and E. Oran, "Spontaneous transition of turbulent flames to detonations in unconfined media," Phys. Rev. Lett., vol. 107, no. 5, p. 54501, 2011.

[11] W. E. Lorensen and H. E. Cline, "Marching cubes: A high resolution 3d surface construction algorithm," *SIGGRAPH Comput. Graph.*, vol. 21, no. 4, pp. 163–169, Aug. 1987.